Cells and Materials

Volume 2 | Number 3 Article 4

1992

Applications of Fourier Transform Infrared (FT-IR) Microscopy to the Study of Mineralization in Bone and Cartilage

Adele L. Boskey
The Hospital for Special Surgery, New York

Nancy Pleshko
Rutgers University, Newark

Stephen B. Doty
The Hospital for Special Surgery, New York

Richard Mendelsohn
Rutgers University, Newark

CELLS AND MATERIALS, Vol. 2, No. 3, 1992 (Pages 209-220) 1051-6794/92$3.00+.00
Scanning Microscopy International, Chicago (AMF O'Hare), IL 60666 USA

APPLICATIONS OF FOURIER TRANSFORM INFRARED (FT-IR) MICROSCOPY TO THE STUDY OF MINERALIZATION IN BONE AND CARTILAGE

Adele L. Boskey*, Nancy Pleshko[1], Stephen B. Doty, and Richard Mendelsohn[1]

The Laboratory for Ultrastructural Biochemistry,
The Hospital for Special Surgery, New York, NY
[1]The Department of Chemistry, Rutgers University, Newark NJ

(Received for publication May 9, 1992, and in revised form October 30, 1992)

Abstract

Knowledge of the phase, composition, and crystallite size and perfection of the mineral in normal and abnormally calcified tissues provides insight into the mechanism by which this mineral was deposited. These data also can be used to develop rational therapies for pathological conditions characterized by abnormal mineral deposition. As illustrated in this review, coupling of an optical microscope with a Fourier transform infrared (FT-IR) spectrophotometer permits the mapping at 20 μm spatial resolution of changes in mineral characteristics (content, particle size, composition) in the growth plate, in bone biopsies, in mineralizing cell culture systems, and in soft tissue calcifications. Based on the infrared properties of apatitic compounds, and comparisons with x-ray diffraction data, correlations have been established from which mineral parameters can be determined. The validity of these spectral correlations has been demonstrated by independent measurements of mineral content (ash weight), and crystal particle size (dark field electron microscopy).

Key words: Fourier transform infrared (FT-IR), infrared spectroscopy, hydroxyapatite, calcified cartilage, bone mineral, FT-IR microscopy, cell culture, osteoporosis.

*Address for correspondence:
Adele L. Boskey
The Hospital for Special Surgery
535 East 70th Street
New York NY 10021
Telephone number: (212) 606-1453
FAX number: (212) 472-5331

Introduction

The mineralized connective tissues consist of a calcium phosphate phase (analogous to the mineral hydroxyapatite, $Ca_{10}(PO_4)_6(OH_2)$) deposited in an organized fashion on an organic matrix. The organic matrix consists predominantly of collagen in all the mineralized tissues with the exception of enamel. Apatite crystal size and perfection (crystallinity) in the calcified tissues vary according to tissue site, tissue function, animal age and pathology. Changes in mineral phase composition, and in crystallinity, may provide insight into the process of biologic mineralization, the aetiology of diseases, and the effects of therapeutic regimens. Characterization of such variation is therefore important both for the developmental biologist and for the design of improved therapies for diseases in which mineral deposition and/or turnover is abnormal, e.g., osteogenesis imperfecta (Vetter *et al.*, 1991), osteomalacia (Boskey, 1985; Boskey *et al.*, 1988a), osteopetrosis (Boskey and Marks, 1985), osteoporosis (Baud *et al.*, 1976, 1988; Cohen and Kitzes, 1981; Thompson *et al.*, 1983), and various forms of dystrophic ossifications (Boskey *et al.*, 1988b).

The crystallinity of the mineralized tissues and of synthetic analogues of the mineral in these tissues has been extensively studied by various chemical and instrumental methods (Blumenthal *et al.*, 1975; Eanes *et al.*, 1973; Fowler *et al.*, 1966; Termine and Lundy, 1973). Most of these studies have involved analyses of homogenized powders, however there are many questions which cannot always be addressed when homogenous samples are examined. Specifically, it is important to know if mineral is present, how much of it there is, where it is localized morphologically, and what is its nature (crystalline phase) and characteristics.

Techniques used to address such questions include light microscopy, electron microscopy (EM), nuclear magnetic resonance (NMR) spectroscopy (Aue *et al.*, 1984), electron spin resonance (ESR) spectroscopy (Doi *et al.*, 1982), and X-ray diffraction and infrared (IR) spectroscopy. While each of these techniques can demonstrate the presence of mineral, light microscopy and EM (without diffraction) do not generally provide information on the nature of the mineral phases present.

X-ray diffraction, NMR, ESR and IR, while enabling identification of the nature of the phases present, do not allow determination of the spatial localization of the mineral phase, or of the relative amounts of mineral and matrix present. Only EM allows direct measurement of the dimensions of mineral crystals; although the Scherrer equation allows a size parameter (dependent on both particle size and crystal perfection) to be calculated from the broadening of isolated peaks in the X-ray powder diffraction pattern of small crystals (Cullity, 1967).

Traditionally, X-ray diffraction is the technique of choice for determination of the particle size of hydroxyapatite (HA) crystals in biologic tissues (Baud *et al.*, 1988; Boskey and Marks, 1985; Vetter *et al.*, 1991). Ground tissue samples are required, however, thereby prohibiting the analysis of morphologic distribution of mineral, or analysis of tissue samples with rapid spatial variation in mineral structure. Microbeam X-ray diffraction can be performed on microscopic sections and has recently been utilized to study the crystallinity of HA in dentin (Abe *et al.*, 1991). However, this technique is not readily available.

Electron microscopy is frequently utilized to study the components of intact calcified tissues (Abe *et al.*, 1991; Arsenault, 1988; Hukins *et al.*, 1986; Moradian-Oldak *et al.*, 1991). Except where high voltage or selected area electron diffraction is used, detailed information about the structure of the mineral phase cannot be obtained, especially in poorly mineralized tissues. Further, this technique is not convenient for mapping the variation in structure of the mineral phase throughout a tissue due to the large number of sections that must be examined. Similarly, X-ray microprobe analysis can provide quantitative analyses of Ca:P ratios (Hukins *et al.*, 1986) but even when compared to standards, these may not reveal the nature of the phases present.

Using light microscopy, histologic and histomorphometric studies are performed to analyze the gross structural characteristics of bone, such as thickness of cortical bone (Kragstrup *et al.*, 1989), or trabecular bone volume (Baud *et al.*, 1988), and, through the use of fluorescent-hydroxyapatite binding dyes, the cellular activity. Although a useful diagnostic technique revealing both the distribution of the mineral and some dynamic parameters describing mineral deposition rates, histomorphometry does not yield specific information about the quality (particle dimensions, purity, etc.), identity, and crystallinity of the mineral phase(s).

Raman microprobe spectroscopy permits evaluation of the structure of the components of normal and pathologically calcified tissues at the microscopic level (Casciani *et al.*, 1979). The main disadvantage of Raman spectroscopy is the inherent interference from the fluorescence arising from the organic matrix of bone and other calcified tissues when subjected to visible or near UV-laser excitation. However, recent innovations in Raman technology have led to the development of an approach whereby the spectrum is excited with near IR radiation at 1.064 μm. The loss in scattering intensity (which goes approximately as the fourth power of the excitation frequency) is overcome by the multiplex advantage of sending the radiation through an interferometer for generation of the frequency spectrum. In addition, the fluorescence is not excited due to the long wavelength. The technique, termed FT-Raman spectroscopy, has not yet been widely applied to biological systems, but may eventually prove to be a useful complement to FT-IR. Typical spectral quality achievable currently in non-microscopic applications are shown in the work of Chioh *et al.* (1991).

Structural information relating to the mineral often is obtained by infrared spectroscopy (Bailey and Holt, 1989). The infrared spectrum can be used to determine the nature of the calcium phosphate phase present (Baddiel and Berry, 1966; Fowler *et al.*, 1966; Fowler, 1974), the crystallinity of the apatite present (Termine and Posner, 1966), and the carbonate content of the mineral (Doi *et al.*, 1982; LeGeros *et al.*, 1968). The current generation of Fourier transform infrared (FT-IR) spectrophotometers provides data of extremely high signal to noise ratio which can be manipulated easily by computer, enabling, for example, subtraction of the spectra of background material, scaling to account for concentration differences, calculation of integrated areas, and analyses of the components of complex overlapping peaks (Bailey and Holt, 1989). FT-IR spectroscopy has been applied to the identification of different mineral phases in soft tissue deposits (McCarty *et al.*, 1983; Fineberg *et al.*, 1990), and in studies of the mechanism of biologic calcification (Sauer and Wuthier, 1988; Satomura *et al.*, 1991; Derfus *et al.*, 1992). Second-derivative spectra can be computed to better define bands, thus facilitating the measurement of peak positions. Fourier deconvolution techniques, through which the width of the spectral peaks may be reduced, thus permitting the separation of overlapping bands into their constituent subbands, have recently been utilized to analyze spectra of both synthetic and biological calcium phosphates (Rey *et al.*, 1989, 1990, 1991). More sensitive than X-ray diffraction, and capable of providing information on the structure of the matrix as well as mineral components, these techniques provide more detailed information on powdered samples than previously were reported using infrared spectroscopy. They do not address the questions of morphologic localization.

By coupling of an optical microscope to an FT-IR spectrometer these spectral methods can be used to evaluate both mineral and matrix characteristics which can be determined at discrete sites within the calcified tissues, at a spatial resolution of 10-20 μm (the diffraction limit of infrared radiation). The FT-IR spectrometer offers several advantages for microscopic measurements, including spectral resolution, excellent signal-to-noise, and ease of sample preparation. Even with these benefits, the application of FT-IR microscopy to biological systems is fairly recent.

Previously, characterization of polymers and their contaminants was the primary application of FT-IR

microscopy (Lang *et al.*, 1988; Li *et al.*, 1992). Biological applications are becoming more common. In 1989, we reported the first application of FT-IR microscopy to the analysis of calcified tissues (Mendelsohn *et al.*, 1989). Recently FT-IR microscopy has also been used to identify carbon monoxide in a single red blood cell (Dong *et al.*, 1988), to study isolated cells from solid human tumors (Benedetti *et al.*, 1990), and to characterize urinary crystals (Daudon *et al.*, 1991).

Here, we review the method of FT-IR microscopy and illustrate several applications for the study of the mineralized connective tissues.

Materials and Methods

FT-IR microscopic data reported in this paper were recorded with a SIRIUS 100 spectrophotometer (Mattson Instruments Inc., Madison, WI), equipped with a Bach-Shearer FT-IR microscope, and a mercury-cadmium telluride detector responsive from 3800-700 wavenumbers (cm^{-1}). Spectra of ground powders mixed with KBr were similarly recorded. Calculations of integrated areas, spectral subtraction, curve-fitting, and other spectroscopic calculations were performed using software supplied by Doug Moffat (National Research Council of Canada, Ottawa). Details of data collection and analysis are presented elsewhere (Pleshko *et al.*, 1991).

Specimens for FT-IR microscopic analyses were either cryo-sections of bones or mineralizing cultures, intact cultures fixed in ethanol, or 5-8 μm thick methacrylate embedded sections of bone. Embedded material was either ethanol or formalin fixed. The soft tissue deposit was a 8 μm thick paraffin embedded section of articular cartilage and subchondral bone. The cell cultures examined were differentiating chick limb bud mesenchymal cell micro-mass cultures, maintained in media which allowed calcification. The phosphate source added to the media from day 2 onward was either inorganic phosphate (Pi) or ß-glycerophosphate (ßGP). Further details of the culture methodology are described in detail elsewhere (Boskey *et al.*, 1992a).

For electron microscopic studies of cartilage mineralization, cultures were treated with 2% paraformaldehyde plus 0.5% glutaraldehyde in 0.05 M cacodylate buffer, pH 7.2 for 4 hours at 4 °C. Samples were embedded in Spurr's resin and thin sections collected on alkalinized water, pH 8.5, to prevent dissolution of crystals from the tissues. Stained and unstained sections were observed in bright field and dark field, at 80 kV, using a Phillips CM-12 transmission electron microscope.

Mineral content was verified by ashing (600 °C) dried bone powders for 24 hours. Mineral content was calculated as ash weight/dry tissue weight. Triplicate analyses were done on each sample. Some of the bone powders analyzed had been separated according to density by density gradient centrifugation (Boskey and Marks, 1985) prior to mineral content and FT-IR analysis.

Data, where replicate determinations were available, are presented as mean ± SD. Comparisons were based on analysis of variance, with p corrected by the Bonferroni correction. Statistical significance was defined as $p \leq 0.05$.

Figure 1. Typical ν_1, ν_3 phosphate spectra of calcium phosphate phases. **A** amorphous calcium phosphate, **B** poorly crystalline hydroxyapatite, **C** well-crystallized hydroxyapatite, **D** brushite, and **E** octacalcium phosphate. Reprinted with permission of Calcif Tissue Int from Mendelsohn *et al.* (1989).

Results

Quantitative FT-IR Analyses

Infrared spectroscopy has long been in use for the identification of calcium phosphate phases (Bailey and Holt, 1989). Comparison of spectra from model compounds characterized by other techniques (e.g., X-ray

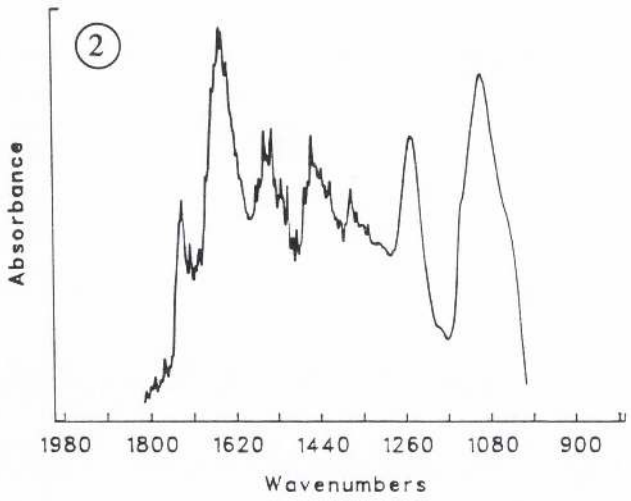

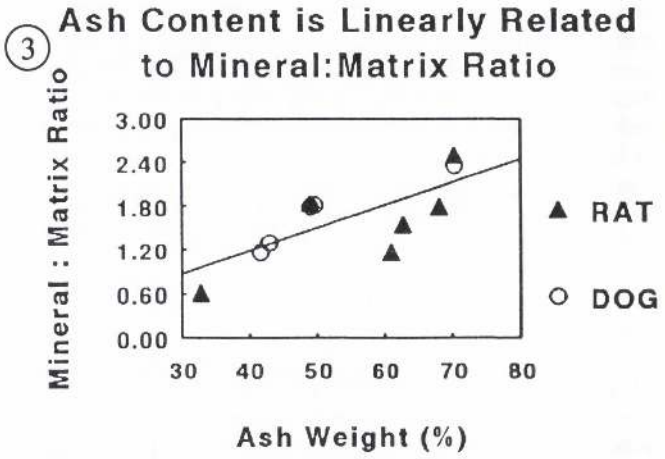

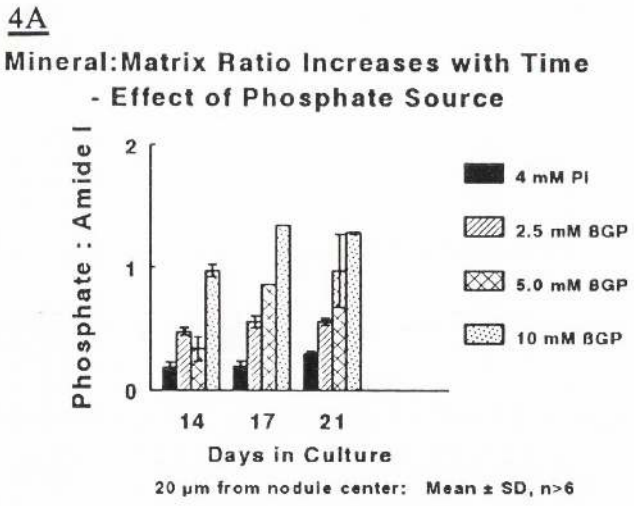

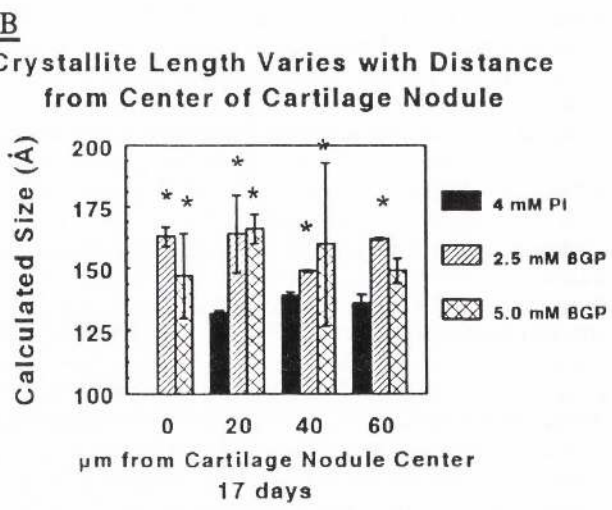

Figure 2. Typical FT-IR spectrum of chick bone. Note the increased intensity of the phosphate band. Reprinted with permission of Bone & Min from Boskey *et al.* (1992a).

Figure 3. Relationship between relative mineral:matrix ratio determined as integrated areas of the phosphate and amide I bands, respectively, and the mineral content as determined by ashing. FT-IR data is based on analyses of powdered tissues in KBr pellets (n = 3 for each point). Line shown is least-squares fit, r = 0.8. Standard deviations for ash weights ≤ 6%; standard deviations for mineral:matrix ratio ≤ 3%.

Figure 4A. Relative mineral:matrix ratios, mean ± SD, in mineralizing cultures as a function of time, for different phosphate sources. ßGP = ß-glycerophosphate, Pi = inorganic phosphate. Adapted from Boskey *et al.* (1992b). At each time point shown ratios with each βGP concentration are significantly greater than those with 4 mM Pi, $p \leq 0.05$.

Figure 4B. Calculated crystallite particle length (mean ± SD) in differentiating mesenchymal cell cultures at day 17 as function of site from center of nodule, in the presence of different phosphate sources. ßGP = ß-glycerophosphate, Pi = inorganic phosphate. Adapted from Boskey *et al.* (1992b). * $p \leq 0.05$ relative to 4mM Pi.

diffraction) to spectra from unidentified deposits have routinely been used to determine the composition of physiologic and dystrophic mineral deposits. Figure 1 presents spectra of the phosphate region (900-1200 wavenumbers (cm^{-1})) of the more frequently encountered calcium phosphate minerals, hydroxyapatite, amorphous calcium phosphate, brushite, and octacalcium phosphate. These spectra were obtained using KBr pellets containing synthetic calcium phosphates previously identified by X-ray diffraction. It is quite apparent how the shape of these peaks can be used to provide "fingerprint" analyses of the mineral phases present.

Figure 2 shows a typical spectrum for bone. The amide I band (1620-1680 cm^{-1}) corresponds primarily to the peptide bond C=O stretch. The amide II mode (1520-1560 cm^{-1}) contains contributions from the C-N stretch and N-H in plane bending coordinates. The relative ratio of the integrated areas of the phosphate band at approximately 1060 cm^{-1} to that of the amide I band is qualitatively related to the mineral content of the tissue and thus provides a means of characterizing microscopic samples in a non-destructive manner. The relationship between this ratio and the gravimetrically determined ash weight for both rat and dog tissues is shown in Figure 3. This qualitative relationship has been used to map (Figure 4A) the changes in mineral content in mineralizing cell cultures as a function of location and time in culture (Boskey *et al.*, 1992b).

Additional information (Pleshko *et al.*, 1991) can be obtained from analysis of the overlapping ν_1, ν_3 phosphate region at 900-1200 wavenumbers (Figure 5A). This complex contour arises primarily from the symmetric (ν_1) and antisymmetric (ν_3) P-O stretching modes. Curve-fit analysis shows the phosphate band consists of six components; inclusion of additional components has little effect on the goodness-of-fit of the calculated contour.

Based on comparisons of such curve-fit parameters with data determined by X-ray diffraction, several useful correlations have been elucidated. On a qualitative basis, the position of the "A" band at approximately 1020 wavenumbers (cm^{-1}) increased with increasing crystallite size. The percent area of a component at approximately 1060 cm^{-1} ("B" band) was found to be related to the particle size (length) and perfection in the long (c-axis) axis direction, by an exponential equation (Pleshko *et al.*, 1991):

$$\text{particle length (Å)} = -30.7\ X^{0.284} + 227.8$$

where X is the % area of the "B" band. This correlation, as demonstrated in Figure 5B, can be used to analyze spectra from a wide range of samples, including homogenized powders and histologic samples.

To assess reproducibility of this curve-fitting methodology, the same spectra have been analyzed and curve-fit multiple times by two independent investigators. No significant ($p \leq 0.05$) changes in calculated particle length were detected.

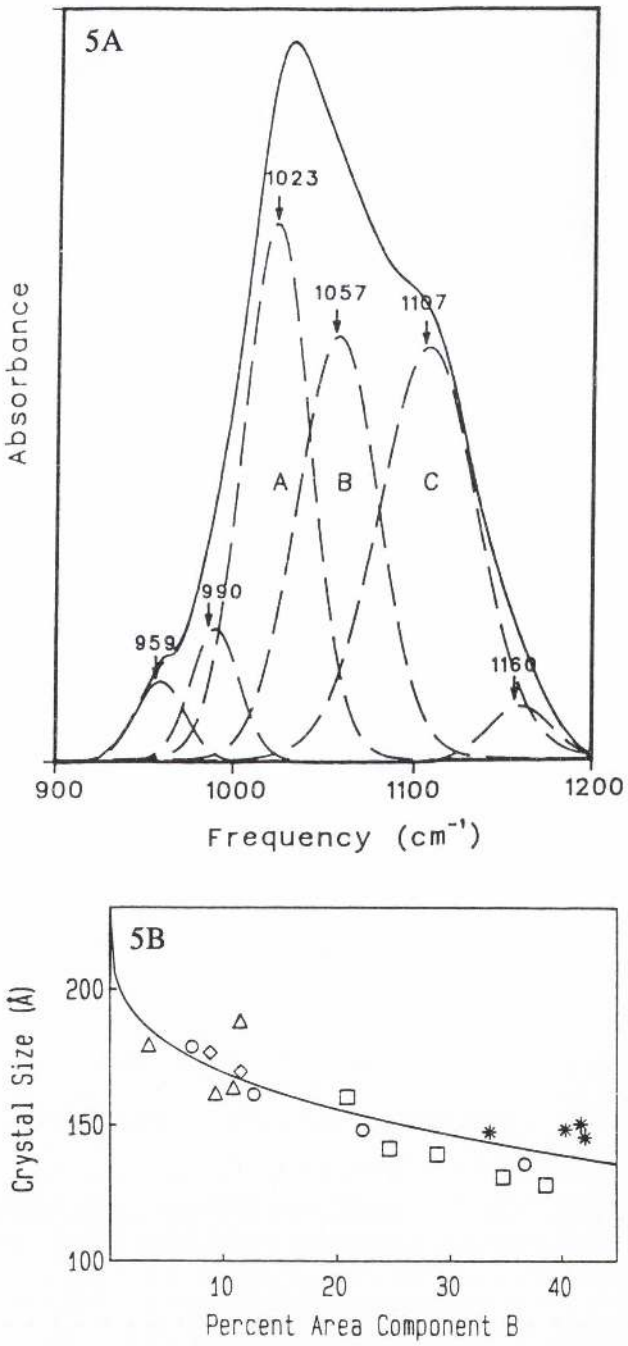

Figure 5A. Curve fit spectra of synthetic carbonate-apatite. Position (cm^{-1}) of each subband (dashes) used to fit the curve is indicated, as are the major bands designated A, B, and C. **Figure 5B**. Correlation between per cent area B band and crystallite size as derived from X-ray diffraction. Measurements were made using a series of synthetic apatites (HA). ○ - HA prepared at pH 8.5; □ - carbonate substituted apatite prepared at pH 8.5, * - carbonate substituted HA prepared at pH 7.4; ◇ - fluoride substituted HA prepared at pH 8.5. ▵ - fluoride substituted HA prepared at pH 7.4. (Reprinted with permission of Biophys J from Pleshko *et al.* (1991).

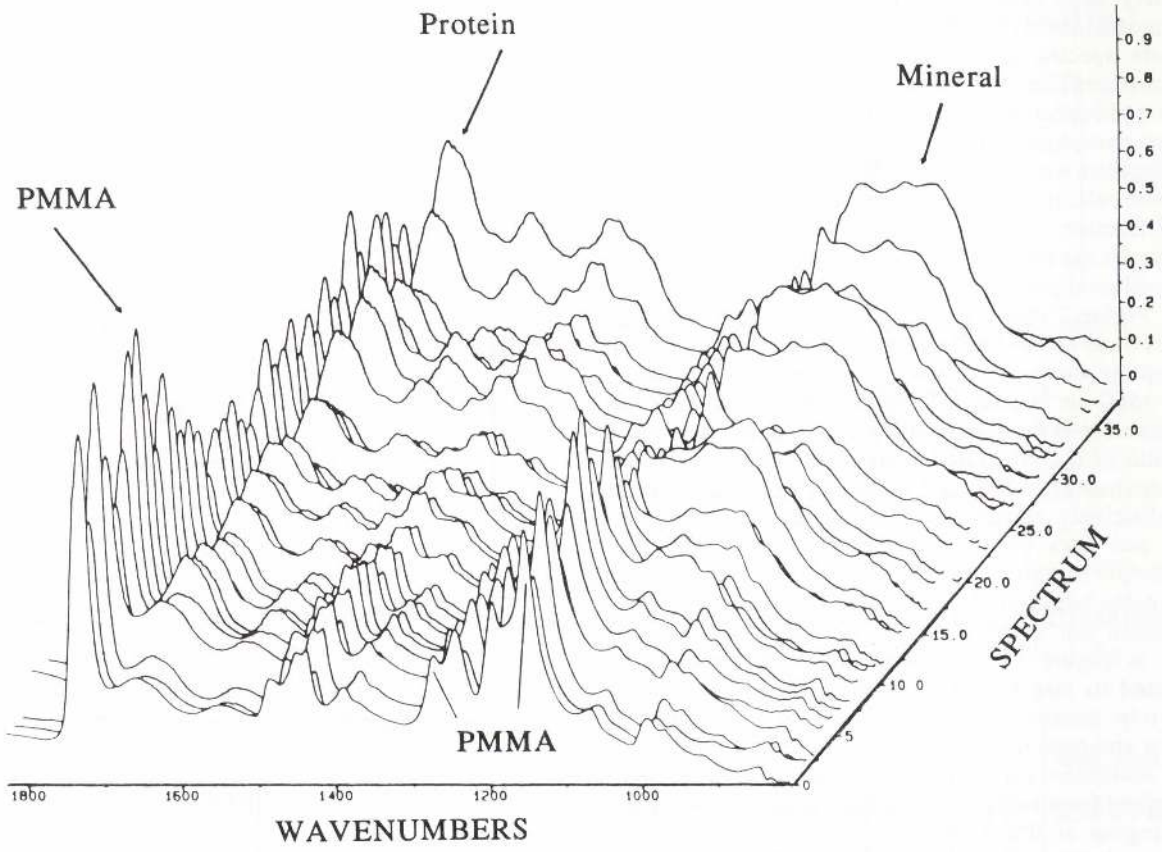

Figure 6. Three-dimensional map of growth plate of rat femur. FT-IR data were obtained by point to point acquisition of data with a 75 μm aperture. Spectrum number is plotted on the y axis, absorbance (Intensity) on the z axis. Specimen had been fixed in polymethyl methacrylate, and absorbance at 1729 wavenumbers comes from carbonyl of that embedding media. Intensities indicate relative amounts of PMMA, protein, and mineral in each region of the femur. The mineral spectra are characteristic of apatite of varying size and perfection and do not show evidence of any non-apatitic phases. [Reprinted with permission from Pleshko NL, Boskey AL, Mendelsohn R (1992) An infrared study of the interaction of polymethyl methacrylate with the protein and mineral components of bone. J Histochem **40**, 1413-1417, Figure 3].

Well crystallized apatites showed a better resolved spectral component at 962 wavenumbers (cm^{-1}) whose relative contribution decreased as crystal size increased from 200-450 Å. This parameter could be used to characterize apatite crystals of larger size.

Applications of FT-IR Microscopy

The growth plate

The suitability of FT-IR microscopy for analysis of mineralized connective tissues was first demonstrated by analysis of the rachitic and normal rat growth plates (Mendelsohn *et al.*, 1989). It is in this area of long bones (the physis or growth plate) in the growing animal that the cartilaginous matrix becomes mineralized and is remodeled and converted into bone. Figure 6 presents a map of the spectral variations in the normal rat growth plate. This map was constructed using a Spectra-Tech IRμS microscope, which provided sequential spectra every 10 μm across a 975 x 225 μm rectangle, starting in the middle of the hypertrophic cell zone, and ending in the metaphyseal bone. As can be seen from this figure, the protein content throughout the growth plate is relatively constant, while the mineral content changes in amount, and in spectral characteristics. The variations in these characteristics are indicative of growth and remodeling, and of alterations in carbonate and acid phosphate content. Thus the initial mineral formed in the

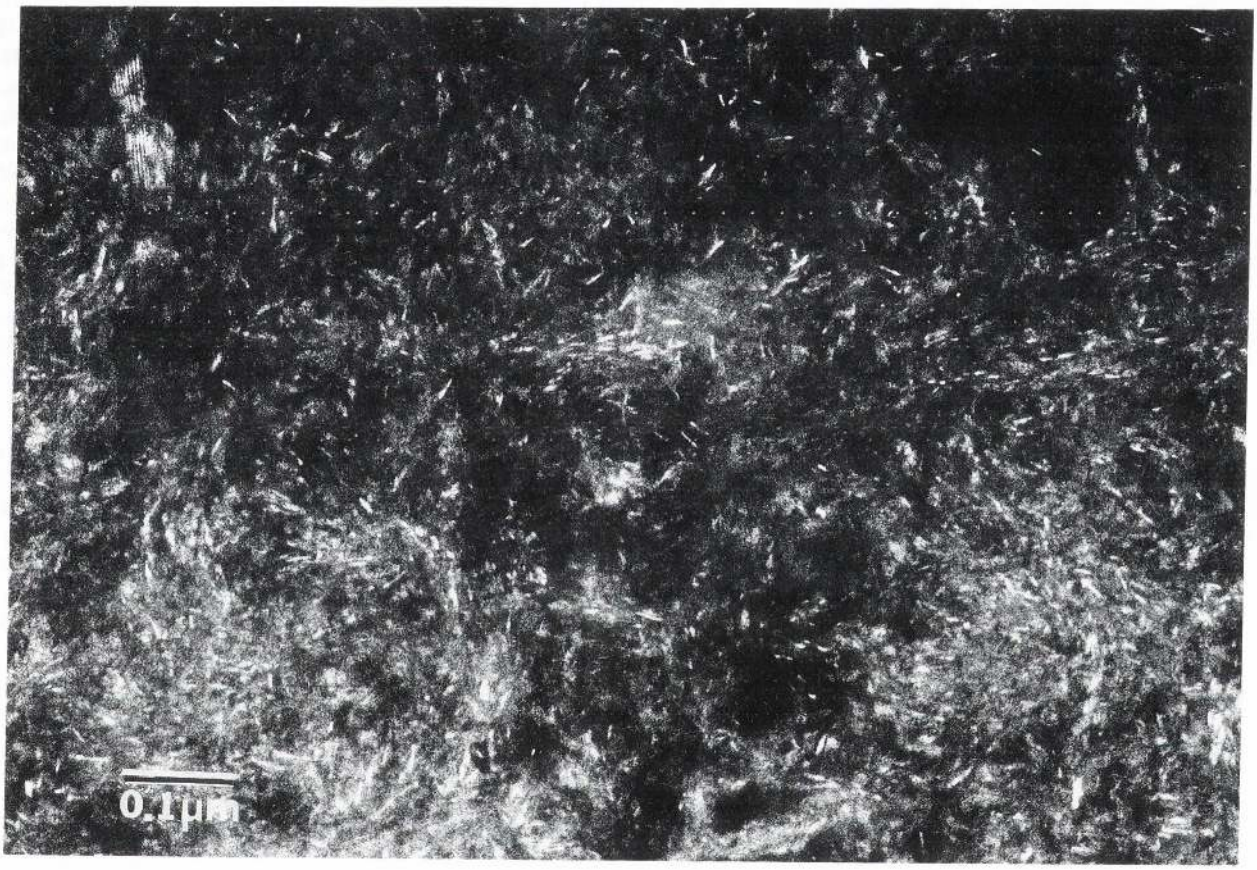

Figure 7. Dark field EM image of a section of a day 14 culture maintained in the presence of 5 mM ß-glycerophosphate. Measurements of 25 crystals in 5 different fields showed crystal lengths ranged from 96-272 Å.

hypertrophic zone of the growth plate shows a spectrum with a broad phosphate peak; as mineralization continues the peak is sharpened (indicative of a change in crystal size). The samples shown in this figure had been fixed in ethanol and embedded in polymethyl methacrylate (PMMA) to allow sectioning. A band due to the presence of PMMA appears in these spectra at 1729 cm^{-1}.

Using such maps coupled with curve-fitting analyses for the study of tissues fixed and preserved in different ways, we have demonstrated that fixation techniques do not alter the properties of the mineral (Pleshko *et al.*, 1992a) although they can have major effects on the protein components, and that PMMA penetrates to a greater extent into the organic than into the mineralized matrix of bone (Pleshko *et al.*, 1992b).

Tissue culture

As indicated above, FT-IR analyses of mineral formed in mineralizing cell cultures has provided insight into both the nature of the mineral present, the relative amount of the mineral, and the crystallinity of the mineral phase. For example, differentiating mesenchymal cell cultures form a cartilaginous matrix when plated at high density, and deposit mineral if cultured in the presence of 3-4 mM inorganic phosphate (Boskey *et al.*, 1992a). Cultures maintained in the presence of inorganic phosphate or ß-glycerophosphate (ßGP) had been noted by X-ray diffraction to produce mineral of different crystallinity, with ßGP-treated cultures having larger/more nearly perfect crystals (Figure 4B). Using FT-IR microscopy, the distribution of large (dystrophic) and smaller (physiologic) mineral crystals was mapped (Boskey *et al.*, 1992b). With quantitative FT-IR microscopy, the mineral crystals at different sites in the matrix in 14 day cultures with 5 mM ß-glycerophosphate ranged size from 150-190 Å (Boskey *et al.*, 1992b). Dark-field electron microscopic imaging of a single EM section of a culture with 5 mM ßGP (Figure 7) showed crystals ranging in length from 96-272 Å, which overlaps the 160

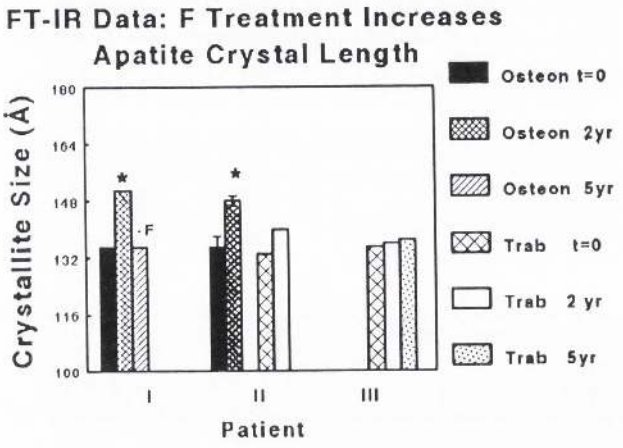

Figure 8. Change in calculated mineral particle size (c-axis direction) with F treatment of three osteoporotic patients. Data represent newest mineral in the cortical bone (osteon) or trabeculae (trab). All patients received F for indicated number of years unless labelled -F. Values are mean ± SD. * $p \leq 0.05$ relative to time 0.

Å determined from the FT-IR data. While the mean length of 201 ± 46 Å (n = 25 crystals), was significantly different from the 160 ± 10 Å determined with the FT-IR data (n = 15 spectra) ($p \leq 0.02$), the number of sections examined (n = 3) may not have permitted sufficient sampling to determine the average crystallite length in the FT-IR section. Such preliminary measurements none-the-less are providing independent evaluation of the FT-IR based spectra-structure correlations.

Changes in Osteoporotic Human Bone

FT-IR microscopy is also being used to map the changes in the mineral in bone biopsies from osteoporotic humans and animals (Boskey, 1990). As summarized in Figure 8, such maps, prepared using histologic sections previously evaluated by histomorphometry, demonstrated fluoride dependent changes in mineral crystal sizes in the cortical bone (and to a lesser extent in the trabecular bone) of osteoporotic patients. The figure contains representative data from 3 patients (I-III). These patients each had multiple iliac crest biopsies taken during the handling of their osteoporosis. Data represent the spectral analysis of three sites in the newest formed osteon (cortical bone) or trabeculae. Values are mean ± standard deviation (SD) from a minimum of 3 spectra. Patient I was treated with NaF for two years and then fluoride treatment was stopped due to a diagnosis of fluorosis. The third biopsy was obtained five years after NaF treatment was discontinued. The second patient was also treated with NaF for two years before the second biopsy. The third patient received fluoride for five years with biopsy material available at years two and five. Fluoride, as reported earlier based on X-ray diffraction data, caused an increase in the average particle length (Gron *et al.*, 1966; Baud *et al.*, 1988). This increase in crystal particle size and perfection theoretically is beneficial, as larger/more nearly perfect crystallites tend to be less readily resorbed. What had not been shown before is the relatively small increase in trabecular bone crystallite size, as contrasted with that in the cortical bone. It however is the trabecular bone that appears to be lost to the greater extent in osteoporosis. It is interesting to note that the patient who stopped fluoride treatment had a broader particle size range in her newly formed cortical bone, suggesting new mineral deposition was occurring.

Analysis of dystrophic calcification

One of the potentially useful clinical applications of FT-IR microscopy is the analysis of soft tissue calcifications in tissues in which there are a variety of mineral phases, e.g., demonstrating the presence of oxalate crystals in bone, or identifying dystrophic deposits in soft tissues or subchondral bone. By collecting spectra of the surrounding soft tissue, bone (verified by polarization), and unknown deposits, one can be sure that the deposit being analyzed is not bony debris. We have recently used FT-IR microscopy to identify the presence of poorly crystalline apatite not associated with a collagenous matrix in the subchondral bone of a person with avascular necrosis. As seen in Figure 9, the spectrum was distinct from that of the adjacent bone (which did polarize light, whereas the deposit did not), enabling us to verify that the deposit was not bone debris. The spectra did not show the presence of any non apatitic phases, but was characteristic of a poorly crystalline apatite. Curve-fit analysis of the mineral in the deposit was used to demonstrate that the particles were of crystal sizes smaller than those in bone mineral.

Discussion and Conclusions

Infrared spectroscopy has been widely used to characterize the mineral in normal and dystrophic deposits. The technique compliments X-ray diffraction and electron microscopic analysis. Using any of these techniques, however, it is difficult to indicate how mineral properties change with morphology. The coupling of a light microscope to the FT-IR spectrophotometer allows spectra to be measured at discrete sites within the tissue. The spectra can be recorded with high signal to noise ratios, and manipulated to provide quantitative information on both mineral and matrix. Spectra can be collected in intact tissues, in cryo-sections, and in thin sections of fixed tissues. Following data collection, sections can be stained to allow identification of specific markers, examined by back-scatter electron imaging, or further sectioned for electron microscopy. Development of special culture dishes which are optically inert, should also allow monitoring of changes in spectral characteristics during the process of cell mediated mineralization.

Using FT-IR microscopy we have demonstrated that the characteristics of the mineral deposited within the growth plate change with time, that mineral properties can be determined in fixed, as well as in fresh tissues, and that predictions based on correlations between FT-IR analyses and X-ray diffraction are in agreement with those determined by electron microscopy. Applying these techniques to mineralizing cartilage cultures, we have demonstrated that the first detectable mineral is a poorly crystalline apatite, that crystal size increases with time in culture, and with distance from the central of the cartilage nodule. Further we have shown that treating the cultures with ßGP results in some mineral which appears dystrophic in crystal size and site (Boskey *et al.*, 1992b). Since measurements can be made in biopsy sections, FT-IR microscopy also provides a powerful technique for characterizing mineral deposits in normal and diseased tissues.

Acknowledgements

This work was supported by NIH grants DE04141 and AR037661 (ALB) and by the Busch bequest to Rutgers University (RM). The authors would like to thank Dr. Bullough, Dr. Bansal, and Dr. DiCarlo, of the Department of Pathology at the Hospital for Special Surgery, for their contributions to this study.

References

Abe K, Masatomi Y, Moriwaki Y, Ooshima T (1991) X-ray diffraction analysis and transmission electron microscopic examination of globular dentin. Calcif Tissue Int **48**, 190-195.

Arsenault AL (1988) Crystal-collagen relationships in calcified turkey leg tendons visualized by selected-area dark field electron microscopy. Calcif Tissue Int **43**, 202-212.

Aue WP, Roufosse AH, Glimcher MJ, Griffin RG (1984) Solid state phosphorus nuclear magnetic resonance study of synthetic solid phase of calcium phosphate; potential models of bone mineral. Biochem **23**, 6110-6114.

Baddiell CB, Berry EE (1966) Spectra structure correlations in hydroxy and fluoroapatite. Spectrochim acta **22**, 1407-1416.

Bailey RT, Holt C (1989) Fourier transform infrared spectroscopy and characterisation of biological calcium phosphates. In: Calcified Tissue, Hukins DWL (ed.), Macmillan Press, Houndsmills, England, chap. 5.

Baud CA, Pouëzat JA, Tochon-Danguy HJ (1976) Quantitative analysis of amorphous and crystalline bone tissue mineral in women with osteoporosis. Calcif Tissue Res **21s**, 452-456.

Baud CA, Very JM, Courvoisier B (1988) Biophysical study of bone mineral in biopsies of osteoporotic patients before and after long-term treatment with fluoride. Bone **9**, 361-365.

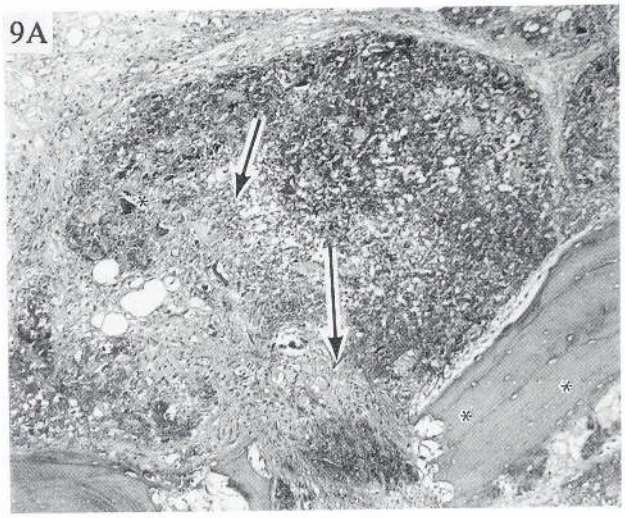

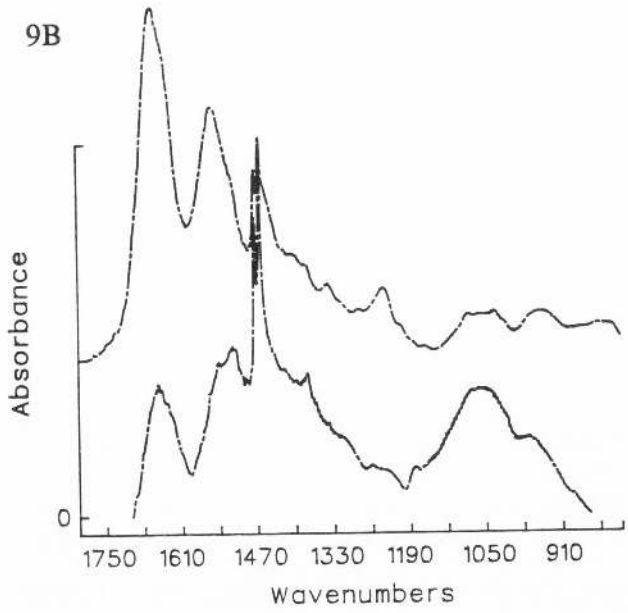

Figure 9. Analysis of pathologic deposit.

Fig. 9A (top). Histologic section showing non-polarizing mineral deposits (arrow) and bone (*).

Fig. 9B (bottom). FT-IR spectra of bone matrix (top spectrum) and apatitic deposit (lower spectrum). A poorly mineralized area of the bone matrix was sampled, hence the low mineral:matrix ratio. Note that the dystrophic deposit was associated with very little protein, as indicated by the relative absorbance of the Amide I and Amide II bands. The bands at 1470-1450 cm^{-1} are due to the paraffin in the sample.

Benedetti E, Teodori L, Trinca ML, Vergamini P, Salvati F, Mauro F, Spremolla G (1990) A new approach to the study of human solid tumor cells by means of FT-IR microspectroscopy. Applied Spec **44**, 1276-1280.

Blumenthal NC, Betts F, Posner AS (1975) Effect of carbonate and biological macromolecules on formation and properties of hydroxyapatite. Calcif Tissue Res **18**, 81-90.

Boskey AL (1985) Lipid changes in the bones of the healing vitamin D deficient, phosphate deficient rat. Metab Bone Dis & Rel Res **6**, 173-178.

Boskey AL (1990) Bone mineral and matrix: Are they altered in osteoporosis? The Orthopedics Clinics of North America **21**, 19-29.

Boskey AL, Marks SC (1985) Mineral and matrix alterations in the bones of incisors-absent (ia/ia) osteopetrotic rat. Calcif Tissue Int **37**, 287-292.

Boskey AL, DiCarlo EF, Gilder H, Donnelly R, Wientroub S (1988a) The effect of short-term treatment with vitamin D metabolites on bone lipid and mineral composition in healing vitamin D-deficient rats. Bone **9**, 309-318.

Boskey AL, Vigorita V, Bullough PG (1988b) Calcium-acidic phospholipid-phosphate complexes: Promoter of mineralization common to pathologic hydroxyapatite-containing calcifications. Am Jour Pathol **133**, 22-29.

Boskey AL, Stiner D, Leboy P, Doty S, Binderman I (1992a) Optimal conditions for cartilage calcification in differentiating chick limb-bud mesenchymal cells. Bone & Min **16**, 11-37.

Boskey AL, Pleshko Camacho N, Mendelsohn R, Doty SB, Binderman I (1992b) FT-IR microscopic mappings of early mineralization in chick limb bud mesenchymal cell cultures. Calcif Tissue Int **51**, 443-448.

Casciani F, Etz ES, Newbury DE, Doty SB (1979) Raman microprobe studies of two mineralizing tissues: Enamel of the rat incisor and the embryonic chick tibia. Scanning Electron Microsc. **1979**; II, 383-391.

Chioh SH, Lee BS, Chang CC, Yu NT (1991) Structural analysis of phospholipase A^2 by near-IR Fourier transform Raman spectroscopy. Biochem Intern **25**, 387-395.

Cohen L, Kitzes R (1981) Infrared spectroscopy and magnesium content of bone mineral in osteoporotic women. Israel J Med Sci **17**, 1123-1125.

Cullity BD (1967) Elements of X-ray Diffraction. Addison-Wesley Publ. Co., Reading, MA, page 99.

Daudon M, Marfisi C, Lacour B, Bader C (1991) Investigation of urinary crystals by Fourier transform infrared microscopy. Clin Chem **37**, 83-87.

Derfus BA, Rachow JW, Mandel NS, Boskey AL, Buday M, Kushnaryov VM, Ryan LM (1992) Articular cartilage vesicles generate calcium pyrophosphate dihydrate-like crystals *in vitro*. Arthritis Rheum **35**, 231-240.

Doi Y, Moriwaka Y, Aoba T, Takahashi J, Joshim K (1982) ESR and IR studies of carbonate containing hydroxyapatites. Calcif Tissue Int **34**, 178-181.

Dong AC, Messerschmidt RG, Reffner JA, Caughey W (1988) IR spectroscopy of a single cell: The human erythrocyte. Biochem Biophys Res Comm **156**, 752.

Eanes ED, Termine JD, Nylen MU (1973) An electron microscopic study of the formation of amorphous calcium phosphate and its transformation to crystalline apatite. Calcif Tissue Res **12**, 143-158.

Fineberg J, Boachie-Adjei O, Bullough PG, Boskey AL (1990) The distribution of calcific deposits in the intervertebral discs of the lumbosacral spine. Clin Orthoped **253**, 32-39.

Fowler BO (1974) Infrared studies of apatites. I. Vibrational assignments for calcium, strontium and barium hydroxyapatites utilizing isotopic substitution. Inorg Chem **13**, 194-207.

Fowler BO, Moreno EC, Brown WE (1966) Infrared spectra of hydroxyapatite, octacalcium phosphate and pyrolysed octacalcium phosphate. Arch oral Biol **11**, 477-492.

Gron P, McCann HG, Bernstein D (1966) Effect of fluoride on human osteoporotic bone mineral. A chemical and crystallographic study. J Bone Jt Surg **48A**, 892-898.

Hukins DWL, Cox AJ, Harries JE (1986) EXAFS characterisation of poorly crystalline deposits from biological systems in the presence of highly crystalline material. J Physique **48**, 1181-1184.

Kragstrup J, Shijie Z, Mosekilde L, Melsen F (1989) Effects of sodium fluoride, vitamin D, and calcium on cortical bone remodeling in osteoporotic patients. Calcif Tissue Int **45**, 337-341.

Lang PL, Katon JE, Bonanno AS, Pacey GE (1988) The identification and characterization of polymer contaminants by infrared microscopy. In: Infrared Microspectroscopy Theory and Applications. Messerschmidt RG, Harthcock MA (eds.), Marcel Dekker, NY, pages 41-72.

LeGeros RZ, Trautz OR, LeGeros JP, Klein E (1968) Carbonate substitution in the apatitic structure. Bull Soc Chim Fr, 1712-1718.

Li S, Nagy EV, Wood BA (1992) Chemical degradation of polyethylene in hip and knee replacements. Trans Orthopaed Res Soc **17**, 41 (abstract).

Mendelsohn R, Hassenkhani A, DiCarlo E, Boskey AL (1989) FT-IR Microscopy of endochondral ossification at 20μ spatial resolution. Calcif Tissue Int **44**, 20-24.

McCarty DJ, Lehr JR, Halverson PB (1983) Crystal populations in human synovial fluid. identification of apatite, octacalcium phosphate, and tricalcium phosphate. Arthritis & Rheum, **26**, 1220-1224.

Moradian-Oldak J, Weiner S, Addadi L, Landis WJ, Traub W (1991) Electron imaging and diffraction study of individual crystals of bone, mineralized tendon, and synthetic carbonate apatite. Connect Tissue Res **25**, 219-228.

Pleshko N, Mendelsohn R, Boskey A (1991) A novel IR spectroscopic method for the determination of

crystallinity of hydroxyapatite minerals. Biophys J **60**, 786-793.

Pleshko NL, Boskey AL, Mendelsohn R (1992a) An FT-IR microscopic investigation of the effects of tissue preservation on bone. Calcif Tissue Int **51**, 72-77.

Pleshko NL, Boskey AL, DiCarlo E, Mendelsohn R (1992b) An infrared study of the interaction of polymethyl methacrylate with the protein and mineral components of bone. J Histochem Cytochem **40**, 1413-1417.

Rey CC, Collins B, Goehl T, Dickson IR, Glimcher MJ (1989) The Carbonate environment in bone mineral. A resolution-enhanced Fourier transform infrared spectroscopy study. Calcif Tissue Int **45**, 157-164.

Rey C, Shimizu M, Collins B, Glimcher MJ (1990) a Resolution-enhanced Fourier transform infrared spectroscopy study of the environment of phosphate ions in early deposits of a solid phase of calcium-phosphate in bone and enamel, and their evolution with age. I: Investigations in the v4 PO_4 domain. Calcif Tissue Int **46**, 384-394.

Rey C, Shimizu M, Collins B, Glimcher MJ (1991) Resolution-enhanced Fourier transform infrared spectroscopy study of the environment of phosphate ions in early deposits of a solid phase of calcium-phosphate in bone and enamel, and their evolution with age. 2: Investigations in the v3 PO_4 Domain. Calcif Tissue Int **49**, 383-388.

Satomura K, Hiraiwa K, Nagayama M (1991) Mineralized nodule formation in rat bone marrow stromal cell culture without ß-glycerophosphate. Bone & Min **14**, 41-54.

Sauer GR, Wuthier RE (1988) Fourier transform infrared characterization of mineral phases formed during induction of mineralization by collagenase-released matrix vesicles. J Biol Chem **263**, 13718-13723.

Termine JD, Lundy DR (1973) Hydroxide and carbonate in rat bone mineral and its synthetic analogues. Calcif Tissue Res **13**, 73-82.

Termine JD, Posner AS (1966) Amorphous/crystalline inter-relationship in bone mineral. Calcif Tissue Res **6**, 335-342.

Thompson DD, Posner AS, Laughlin WS, Blumenthal NC (1983) Comparison of bone apatite in osteoporotic and normal eskimos. Calcif Tissue Int **35**, 392-393.

Vetter U, Eanes ED, Kopp JB, Termine JD, Gehron Robey P (1991) Changes in apatite crystal size in bones of patients with osteogenesis imperfecta. Calcif Tissue Int **49**, 248-250.

Discussion with Reviewers

C.C. Rey: The main questions concern the empirical relationship discovered by the authors between curve fitting results and the length of mineral crystals. Do they have any explanations and/or theoretical support for the existence of such a relationship which is extensively used all over their work?

Authors: The analysis of IR spectra of mineralizing tissues in terms of structural/molecular parameters such as crystal size and/or perfection is a complex subject, not readily addressed by the traditional methods of analysis of molecular vibrational spectra of either monomeric polymeric or crystalline systems (e.g., normal coordinate calculations, dispersion curve construction, factor group analysis, etc.). Thus, in these initial forays into the area, and in an attempt to achieve an interpretation beyond the "zeroth" order, we have relied on empirical methods. When suitable spectra-structure correlations have been generated, then an appropriate (theoretical) framework for their integration may be discerned. Without the availability of empirical data, the problem is absolutely unapproachable. In the current case, our major finding is that the same empirical correlation between the "B" band and crystal size (as defined in the text) appears to be applicable to both (macroscopic minerals formed *in vitro*) and microscopic (tissue) specimen spectra. This is a major step as will enable us to consider (at the appropriate time) suitable frameworks for the simpler (*in vitro*) spectra which will then be transferable to the more complex cases.

C.C. Rey: IR band broadening and band resolution in solids depends on many factors and not only on the size of the crystals (bands shifts corresponding to crystals with slightly different composition, crystal defects, heterogeneities of composition in the same crystal, particulate sizes and Christiansen effect, etc...). Some of these factors affect also the width of X-ray diffraction bands. Can all these factors be neglected in biological apatites?

Authors: Professor Rey's comments address appropriate and well-known concerns about effects of particle size on IR spectral parameters. The presence of reflecting surfaces (in a medium with discontinuities in refractive index) creates substantial analytical and theoretical difficulties. In addition, problems with early generations of IR Microscope technology may create further optical spectral distortions. Whether these factors can be ignored in biological specimens is the subject of ongoing concern in our laboratory. It is certain that transmission spectroscopy of thin sections (as we have used) is a much better means of analysis than reflection spectroscopy, which is otherwise tempting as it avoids some technical aspects of sample preparation. In addition, our microscopic samples are usually sampled at a consistent thickness, and the mineral cross-sectional areas that are studied are larger than the instrument aperture. This gives us some cause to believe that any spectral distortions will at least be fairly consistent within a given sample.

We note that the problems alluded to by Professor Rey have not yet been addressed in any substantive way in the biophysical literature. Clearly the time is appropriate for such studies.

C.C. Rey: The relationship between the mineral/matrix ratio and the ash weight is not convincing at all. Two

reasons may be advanced: 1) the band at 1620-1680 cm^{-1} is also due to water contained in biological samples (possibly associated with apatites even when tissues are fixed) and might not be the best choice for such a determination, and 2) carbonates are partly lost from the mineral during ashing therefore the weight loss does not represent only the organic part of bone.

Authors: The reasonable but admittedly imperfect correlation between the mineral/matrix ratio and relative intensities of the phosphate/Amide I bands, is again (see above) the first step toward a much more quantitative analysis of the spectra. However, it ought to be recalled that the IR method proposed in the current work for the analysis of microscopic sections (which are obviously not amenable for ashing), is the only one around for even crudely estimating the relative amounts of inorganic to organic material at 5 μm spatial resolution. We report these relative values as the ratio of integrated areas for each spectrum and do not claim that we can monitor absolute mineral content. The correlation in Figure 3 is presented to show that we can discriminate between materials with variable mineral contents. As instrumentation improves there are several means by which we can (and will) generate more specific correlations. The presence in the spectra of non-overlapped bands due to carbonate, protein and perhaps even non-proteinaceous organic material in addition to the phosphate will enable us to determine the relative spatial concentrations of each of these species in a rapid and non-destructive manner.

M. Daudon: The authors argue for the relation between the crystal size and the percent area of the B band obtained from apatite spectra using the curve-fitting procedure. It is a very important point. Infrared spectroscopy is well known as a useful technique for differentiating between well crystallized and poor crystalline apatite materials. In cases of mixtures of amorphous calcium phosphate and apatite crystals, it is not sure that the curve-fitting analysis could give a correct measurement of the crystal size of apatite material. Figure 5A does not show evidence that a correlation exists between the B band and the crystal size of carbonate apatite at physiological pH values. In contrast, on Figure 9B, there is evidence that dystrophic deposits are mainly made of either amorphous or poorly crystalline phosphate whereas the poorly mineralized area of the bone matrix mainly contains well crystallized carbonate apatite. As expected, the mean size of crystals (Fig. 7) determined by electron microscopy was higher than the mean value obtained from infrared spectra. Another point is the broad overlapping of the B band with both A and C bands. Thus, the authors should give more convincing data about the reliability of the percent area of the B band and the size of the crystals.

Authors: Professor Daudon indicates that it is unsure whether the curve-fitting analysis could give a correct measurement of the size of an apatite material. The data in Figure 4B, however, point to an indication that such a correlation is applicable to both macroscopic and microscopic samples. We appreciate that there are many technical aspects which are as yet incomplete. Have we addressed all the relevant variables? Is the curve-fitting algorithm we are using the best way to approach the data reduction? The answers to these and related issues must await better technology which can generate the highest possible signal/noise levels in the spectra. Nevertheless, the data have been established with a standard method (X-ray diffraction) and compared with data obtained with a second, independent method (electron microscopy). Thus, we are confident that our initial steps have made substantial inroads into the problem. In terms of the comment about more convincing data, we feel that the data displayed are quite impressive, encompassing, as they do, a wide range of samples.

M. Daudon: Using the curve fitting procedure, the C band at 1107 cm^{-1} shows greater variations in the per cent area than the B band when apatites with different crystalline states are compared. Have the authors investigated the significance of the C band in the apatite structure?

Authors: We are continuously seeking more precise spectra-structure correlations. The "B" band index of crystallinity/size is the most robust to date. The spectral analysis is of course ongoing and the relevance of changes in the "C" band are currently being investigated.